Catalytic Activity Trends of Oxygen Reduction Reaction for Nonaqueous Li-Air Batteries

Yi-Chun Lu,[†] Hubert A. Gasteiger,[*,‡,§] and Yang Shao-Horn[*,†,‡]

[†]Department of Materials Science and Engineering and Electrochemical Energy Laboratory, Massachusetts Institute of Technology, 77 Massachusetts Avenue, Cambridge, Massachusetts 02139, United States

[‡]Department of Mechanical Engineering and Electrochemical Energy Laboratory, Massachusetts Institute of Technology, 77 Massachusetts Avenue, Cambridge, Massachusetts 02139, United States

[§]Current address: Department of Chemistry, Technische Universität München, Lichtenbergstrasse 4, D-85747 Garching, Germany.

* *shaohorn@mit.edu*
hubert.gasteiger@tum.de

Supporting Information

The stability and reversibility of $O_2/O_2^{-\bullet}$ on Pt in 1,2-dimethoxyethane (DME)

To investigate the stability and reversibility of $O_2/O_2^{-\bullet}$ on Pt in 1,2-dimethoxyethane (DME), we examine the oxygen reduction reaction on the Pt disk in 0.5 M $TBAClO_4$ DME as shown in Figure S1. Two observations are noted. First, no reaction current was observed in the range of 3.1 – 2.0 V_{Li} (the potential window used in this study), which suggests that there was no significant reaction associated with Pt, oxygen and DME solvent. Second, the $O_2/O_2^{-\bullet}$ redox couple is stable and reversible even at a slow scan rate of 5 mV s^{-1}. This suggests that O_2^- radical is reasonably stable on Pt electrode in DME.

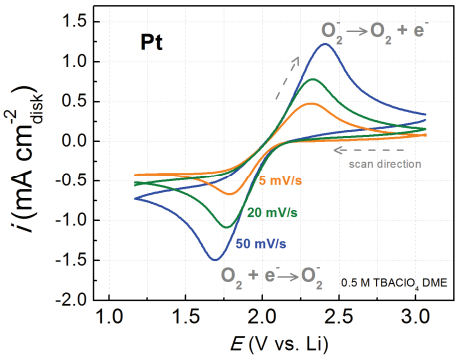

Figure S1. Steady-state cyclic voltammogram of ORR on a Pt disk in O_2-saturated 0.5 M $TBAClO_4$ DME at 5, 20, and 50 mV s^{-1} and 0 rpm.

The poisoning effect of DME

To investigate the poisoning effect of DME molecules on the catalyst surfaces (e.g., Pt disk), we examine the ORR activity of the Pt disk in 0.1 M KOH in the presence of 100 mM DME. The results are compared to that in the pure 0.1 M KOH. Figure S2 shows the polarization curves of ORR on a Pt disk in 0.1 M KOH (orange) and 100 mM DME - 0.1 M KOH (blue) at 10 mV s^{-1} and 900 rpm. We note that the Pt ORR activity is barely influenced by the presence of DME. The difference is 7 mV at 1 mA cm^{-2}_{disk}.

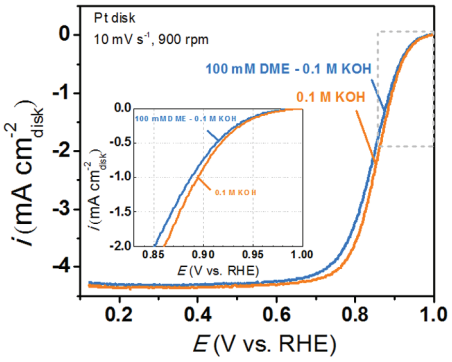

Figure S2. Polarization curves (positive-going scans) of ORR on a Pt disk in 0.1 M KOH (orange) and 100 mM DME - 0.1 M KOH (blue) at 10 mV s^{-1} and 900 rpm.

Rotating disk electrode measurements

Bulk disks

Three-electrode cells were prepared by following procedures. Polycrystalline palladium (Pd), platinum (Pt), gold (Au), glassy carbon (GC) (0.196 cm^2 disks; Pine, USA), and ruthenium (Ru) (0.196 cm^2 disks; Princeton Scientific Corp., USA) surfaces were polished to a 0.05 μm mirror-finish, ultra-sonicated in de-ionized water (18.2 MΩ·cm, Millipore) for 10 min and followed by vacuum-drying at 75°C for 12 hours before each experiment. All electrodes were kept in the vacuum oven and directly transferred to a water-free glovebox (H_2O < 0.1 ppm, Mbraun, USA) without exposing to the ambient. The three-electrode cell used for RDE measurements consists of a lithium-foil counter electrode, a reference electrode based on a silver wire immersed into 0.1 M $TBAPF_6$ (Sigma-Aldrich) and 0.01 M $AgNO_3$ (BASi) in DME which was calibrated against Li metal in 0.1 M $LiClO_4$ DME (0 $V_{Li} \approx -3.64 \pm 0.01$ V vs. Ag/Ag^+), and a bulk disk as the working electrode. The RDE experiments were performed in the water-free glovebox. The electrolyte was 0.1 M $LiClO_4$ DME (H_2O < 20 ppm Novolyte, USA). The working electrode was immersed into an Ar-purged electrolyte for 15 minutes prior to each cyclic voltammetry (CV) experiment. After steady-state CVs were obtained in Ar (2 - 3.15 V_{Li} at 100 rpm, 20 mV s^{-1}), the potential was scanned between 3.15 – 3.0 V_{Li} at 100 rpm, 20 mV s^{-1} for 20 cycles followed by 1 cycle between 3.15 –

2.0 V_{Li} at 100 rpm, 20 mV s^{-1} (the Ar background scan used for capacity correction). Subsequently, the cell was purged with O_2 for 15 min with potential cycling between 3.0 – 3.15 V_{Li}, and then the potential was scanned from 3.15 V_{Li} to 2.0 V_{Li} at 100 rpm, 20 mV s^{-1}. The capacitive-corrected ORR currents were obtained by subtracting the current measured under Ar from that found in pure O_2 under identical scan rates, and rotation speeds as shown in Figure S3. The IR-correction was performed by considering the total cell resistance of 3.1 KΩ measured by EIS.

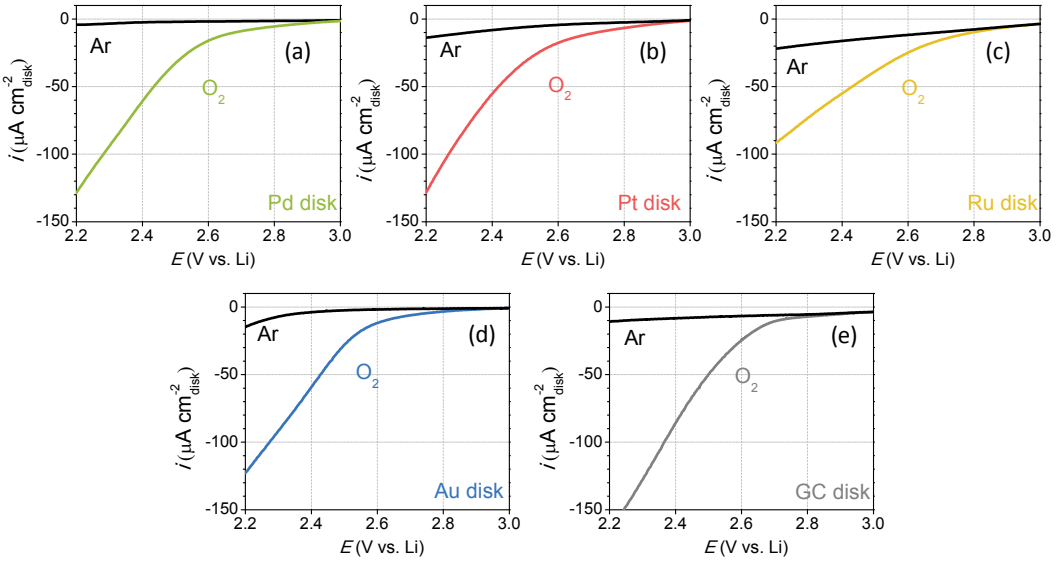

Figure S3. Polarization curves in Ar (steady-state) and in O_2 (1st scan) during the negative-going scan of polycrystalline (a) Pd, (b) Pt, (c) Ru, (d) Au, and (e) GC disks in 0.1 M $LiClO_4$ DME 20 mVs^{-1} and100 rpm.

Background correction and the degree of self-poisoning on bulk surfaces at 2 μA cm^{-2}_{true}

To obtain a reliable intrinsic nonaqueous ORR activity of the bulk surfaces, it is necessary to consider the degree of background correction and the self-poisoning due to solid product formation. To balance these two considerations, we select a specific net ORR current density of 2 μA cm^{-2}_{true}, where the self-poisoning is less than 10% of one monolayer solid product formation and the capacitive-correction is less than 50% as shown in Table S1 (based on Figure 1). The monolayer of the solid product is based on a reported value of 200 μC cm^{-2} for LiO_2.[1] It should be noted that this assumption does not imply the formation of LiO_2 for all surfaces but rather represents the most conservative estimation for monolayer product formation since the charge for one monolayer material would be higher for Li_2O_2 ($2e^-/O_2$) and Li_2O ($4e^-/O_2$).

At 2 μA cm^{-2}_{true}	E (V_{Li})	i_{O2} (μA cm^{-2}_{true})	i_{Ar} (μA cm^{-2}_{true})	Capacitive correction i_{Ar}/i_{O2} (%)	Accumulated charge (μC cm^{-2}_{true})	Monolayer fraction (%)
Pd	2.80	-2.6	-0.7	26	10.2	5
Pt	2.72	-2.9	-0.9	32	12.7	6
Ru	2.66	-4.3	-2.3	53	9	5
Au	2.62	-2.3	-0.4	16	11	6
GC	2.56	-2.4	-0.4	18	8	4

Table S1. Capacitive-correction and the self-poisoning evaluation at a specific ORR current of 2 μA cm^{-2}_{true}.

High-surface-area thin film catalysts

Catalyst thin films and three-electrode cells were prepared by following procedures. Glassy carbon disks were polished to a 0.05 μm mirror-finish, ultra-sonicated in de-ionized water (18.2 MΩ·cm, Millipore) for 10 min and followed by vacuum-drying at 75°C for 3 hours before thin film casting. Thin films of Vulcan carbon (VC), 40 wt.% Au/Vulcan (Au/C), 40 wt.% Ru/Vulcan (Ru/C), 40 wt.% Pt/Vulcan (Pt/C), 40 wt.% Pd/Vulcan (Pd/C) (Premetek, USA) were prepared by drop-casting catalyst inks with a Nafion®/carbon weight ratio of 0.5/1 onto a GC disk, yielding carbon loadings of 0.05 mg_{carbon} cm^{-2}_{disk}. The catalyst inks were composed of the high-surface-area catalysts, lithiated Nafion® (LITHion™ dispersion, Ion-Power, USA), and 20% 2 propanol (Sigma-Aldrich) in de-ionized water. The catalyst thin-films were subsequently dried in vacuum at 75°C for 24 hours before testing. All electrodes were kept in the vacuum oven and directly transferred to a water-free glovebox (H_2O < 0.1 ppm, Mbraun, USA) without exposing to the ambient. The description of the three-electrode cell can be found in the previous session (bulk disk). The working electrode was immersed into Ar-purged electrolyte for 15 minutes prior to each CV experiment. After steady-state CVs were obtained in Ar (2 - 3.15 V_{Li} at 900 rpm, 5 mV s^{-1}), the potential was scanned between 3.15 – 3.0 V_{Li} at 900 rpm, 5 mV s^{-1} for 20 cycles followed by 1 cycle between 3.15 – 2.0 V_{Li} at 900 rpm, 5 mV s^{-1} (the Ar background scan used for capacity correction). Subsequently, the cell was purged with O_2 for 15 min with potential cycling between 3.0 – 3.15 V_{Li}, and then the potential was scanned from 3.15 V_{Li} to 2.0 V_{Li} at 900 rpm, 5 mV s^{-1}. The capacitive-corrected ORR currents were obtained by subtracting the current measured under Ar from that found in pure O_2 under identical scan rates, and rotation speeds. The IR-correction was performed by considering the total cell resistance of 3.1 KΩ measured by EIS.

The electrochemical surface area of the bulk electrodes and the high-surface-area catalysts

CVs of bulk disks and high-surface-area thin film electrodes for electrochemical surface area determination

Mirror-polished (0.05 μm mirror-finish) Pt, Pd, and Au disk electrodes and the Nafion-bonded high-surface-area (Pt/C, Pd/C, Au/C) thin film catalysts on GC electrode (0.05 mg_{carbon} cm^{-2}_{disk}) were mounted to a rotator and immersed into 0.5 M H_2SO_4 (Fluka). A spiral Pt wire was employed as the counter electrode, and a saturated calomel electrode (SCE, Analytical Sensor, Inc.) was used as the reference electrode. The potential of SCE with respect to the reversible hydrogen electrode (RHE) was calibrated from RDE measurements of hydrogen oxidation. All the potential values reported in this paper for aqueous media refer to that of the RHE (V_{RHE}). After the electrolyte was bubbled with Ar for half an hour, the (Pt & Pt/C), (Pd & Pd/C), and (Au & Au/C) working electrodes were scanned between 0.045 - 1.20 V_{RHE}, 0.36 - 1.35 V_{RHE}, and 0.44 - 1.7 V_{RHE}, respectively, at a sweep rate of 50 mV s^{-1}, 0 rpm to reach steady state at room temperature. Finally, steady-state CVs were recorded at 10 mV s^{-1} in the same potential ranges.

CO stripping voltammetry of Ru disk and Ru/C[2,3]

Mirror-polished (0.05 μm mirror-finish) Ru disk electrode and Nafion-bonded high-surface-area Ru/C thin film catalysts on GC electrode (0.05 mg_{carbon} cm^{-2}_{disk}) were mounted to a rotator and immersed into 0.5 M H_2SO_4 (Fluka). After the electrolyte was bubbled with Ar for half an hour, steady-state CV of the Ru working electrodes were obtained between 0.05 – 0.95 V_{RHE}, at a sweep rate of 20 mV s^{-1}, 0 rpm. CO was adsorbed by holding the potential at 0.075 V_{RHE} for 3 min in a CO-saturated cell. The electrode was then transferred to an Ar-saturated cell immersed under potential control at 0.075 V_{RHE} followed by potential scan from 0.075 V_{RHE} to 0.95 V_{RHE} at 20 mV s^{-1}.

Determination of electrochemical surface areas (ESA) and the roughness factor of the selected catalysts

The determination of Pt surface area was done as follows: 1) integrating the net (i.e., with double-layer capacitance subtraction) charge formation of hydrogen adsorption region (negative-going scan from 0.4 V_{RHE} – 0.045 V_{RHE}) and hydrogen desorption region (positive-going scan from 0.045 V_{RHE} – 0.4 V_{RHE}). Double-layer capacitance background was assumed by linear-extension from the double-layer region; 2) Average the net charge from hydrogen adsorption and desorption; 3) the averaged net charge (μC) was then divided by the converting factor for Pt surface,[1] 210 μC cm^{-2}, and yield the ESA of Pt. Considering a geometric area of 0.196 cm^2, the roughness factor of the Pt disk was determined to be 3.3. The ESA of Pt/C was determined to be 96 m^2 g^{-1}_{Pt}.

The determination of Pd surface area was done as follows: 1) integrating the net (i.e., with double-layer capacitance subtraction) charge formation of palladium oxides (negative-going scan from 1.00 V_{RHE} – 0.40 V_{RHE}). Double-layer capacitance background was assumed by linear-extension from the double-layer region; 2) the net charge (μC) was then divided by the reported converting factor (i.e., 400 μC cm^{-2} for the potential window being 1.35 V_{RHE})[4] yielding the ESA of Pd. Considering a geometric area of 0.196 cm^2, the roughness factor of the Au disk was determined to be 2.1. The ESA of Pd/C was determined to be 89 $m^2\ g^{-1}_{Pd}$.

The determination of Au surface area was done as follows: 1) integrating the net (i.e., with double-layer capacitance subtraction) charge formation of AuO or $Au(OH)_2$ (negative-going scan from 1.34 V_{RHE} – 0.92 V_{RHE}). Double-layer capacitance background was assumed by linear-extension from the double-layer region; 2) the net charge (μC) was then divided by the reported converting factor (i.e., 350 μC cm^{-2} for the potential window being 1.7 V_{RHE})[5] yielding the ESA of Au. Considering a geometric area of 0.196 cm^2, the roughness factor of the Au disk was determined to be 4.6. The ESA of Au/C was determined to be 27 $m^2\ g^{-1}_{Au}$.

The determination of Ru surface area was done as follows: 1) integrating the net charge formation of CO adsorption (positive-going scan from 0.075 V_{RHE} – 0.95 V_{RHE}); 2) the net charge (μC) was then divided by the reported converting factor (i.e., 420 μC cm^{-2} assuming a 1:1 ratio of CO to each metal site)[3] yielding the ESA of Ru. Considering a geometric area of 0.196 cm^2, the roughness factor of the Au disk was determined to be 4.4. The ESA of Ru/C was determined to be 185 $m^2\ g^{-1}_{Ru}$.

The determination of GC surface area was done as follows: 1) the specific capacitance of carbon (μF cm^{-2}_{carbon}) in 0.1 M $LiClO_4$ DME was determined to be 10.17 μF cm^{-2}_{carbon}, which was estimated from the capacitance of high-surface-area VC (BET: 222 $m^2\ g^{-1}_{carbon}$) (0.05 $mg_{carbon}\ cm^{-2}_{disk}$) in 0.1 M $LiClO_4$ DME. 2) the specific capacitance obtained above is used to calculate the true surface area of GC assuming the specific capacitance of VC is similar to that of GC in the same electrolyte.[6] Considering a geometric area of 0.196 cm^2, the roughness factor of the GC disk was determined to be 16.

ORR on the high-surface-area thin film catalysts normalized to the true surface area of each catalyst

We examined the net ORR current normalized by the true surface area of each catalyst (Figure S4). Assuming that 60% of the catalyst surface is contributed from VC and 40% is contributed from the metal nanoparticles, the true surface area of the catalyst ($A_{catalyst}$) is calculated as follows:

$$A_{catalyst} = 0.6*A_{carbon} + 0.4*A_{metal\ particle}$$

The determination of the electrochemical surface area of the catalysts and VC are described in the previous session.

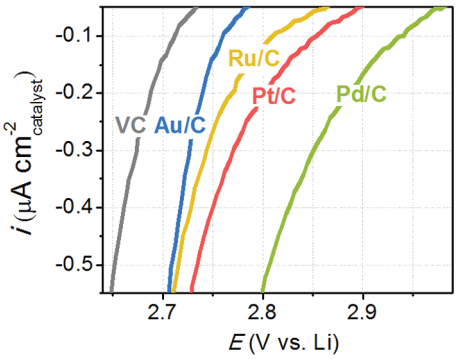

Figure S4. Capacitive and IR-corrected nonaqueous ORR polarization curves normalized by the true surface area of each catalyst for the Pd/C, Pt/C, Ru/C, Au/C and VC thin film RDE in 0.1 M $LiClO_4$ DME 5 mV s^{-1} and 900 rpm.

Li-O_2 cell measurements

Li-O_2 cells consisted of a lithium metal anode (15 mm in diameter and ~0.45 mm thickness) and a lithiated Nafion®-bonded air electrode (12.7 mm in diameter) of either VC, Au/C, Ru/C, Pt/C, Pd/C. Air electrodes with a Nafion®/carbon weight ratio of 0.5/1 were prepared by coating ultrasonicated inks composed of catalyst, lithiated Nafion®, and 2-propanol onto the separator (Celgard C480). After air-drying at 20 °C for 20 minutes, the air electrodes were subsequently vacuum-dried at 75 °C for 3 hours, weighed, vacuum-dried at 75 °C for at least 12 hours prior to transferring into a glovebox (H_2O < 0.1 ppm, O_2 < 0.1 ppm, Mbraun, USA). All electrodes were kept in the vacuum oven and directly transferred to the glovebox without exposing to the ambient. All electrodes were soaked in 0.1 M $LiClO_4$ DME for 12 hours in the glovebox prior to use. The carbon loadings of air electrodes were ≈ 0.4 mg_{carbon} $cm^{-2}_{electrode}$. The average electrode thickness for all electrodes was 20 ± 3 μm. All Li-O_2 single cells were assembled in a glovebox (H_2O < 0.1 ppm, O_2 < 0.1 ppm) with 0.1 M $LiClO_4$ DME as electrolyte and tested at room temperature in the glovebox. Li-O_2 cells were assembled in the following order: 1) placing a lithium foil onto the stainless steel current collector of the cell, 2) adding 50 μl electrolyte, 3) placing two pieces of the separator (Celgard C480, vacuum-dried at 75 °C for at least 12 hours, transferred without exposing to the ambient) onto the lithium foil, 4) adding 50 μl electrolyte, 5) placing the air electrode onto the separator, 6) adding 50 μl electrolyte, 7) placing a current collector (316 stainless steel mesh and spring) on top, and, 8) purging the cell with dry O_2 for 10 minutes in a water-free glovebox (H_2O < 0.1 ppm). Li-O_2 cells were discharged galvanostatically (Solartron 1470) at a rate of 100 mA g^{-1}_{carbon} with a low voltage limit of 2.0 V_{Li}. The full discharge profiles of all Li-O_2 cells are shown in Figure S5.

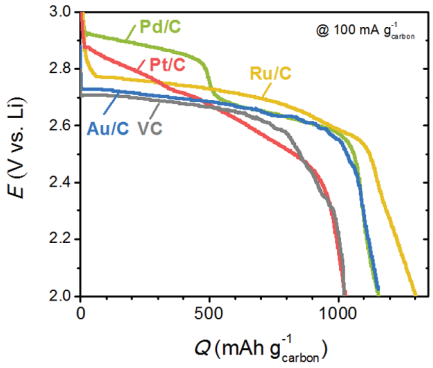

Figure S5. Discharge profiles of VC, Au/C, Ru/C, Pt/C and Pd/C in Li-O_2 cells at 100 mA g^{-1}_{carbon}.

Voltage comparison between high-surface -area RDE and Li-O_2 cells

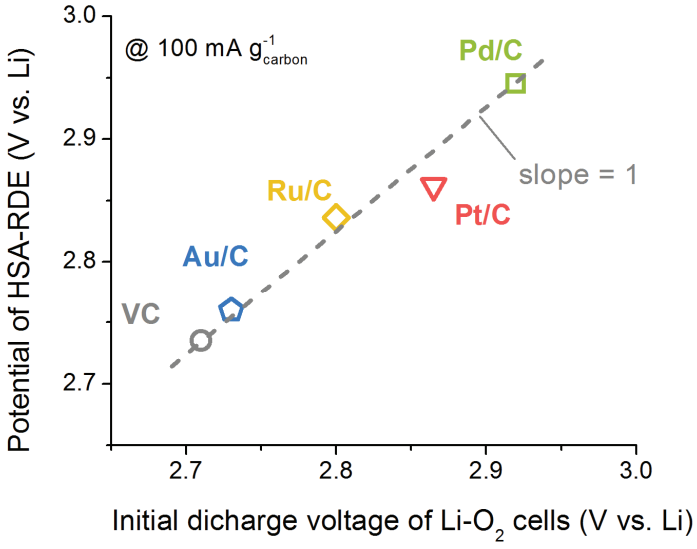

Figure S7. The potentials of the high-surface-area (HSA) thin film RDE at 100 mA g^{-1}_{carbon} as a function of the initial discharge voltages (at Q = 40 mAh g^{-1}_{carbon}) of the Li-O_2 cells at 100 mA g^{-1}_{carbon}.

Previous proposed ORR mechanism for Li^+-containing nonaqueous solvents[7]

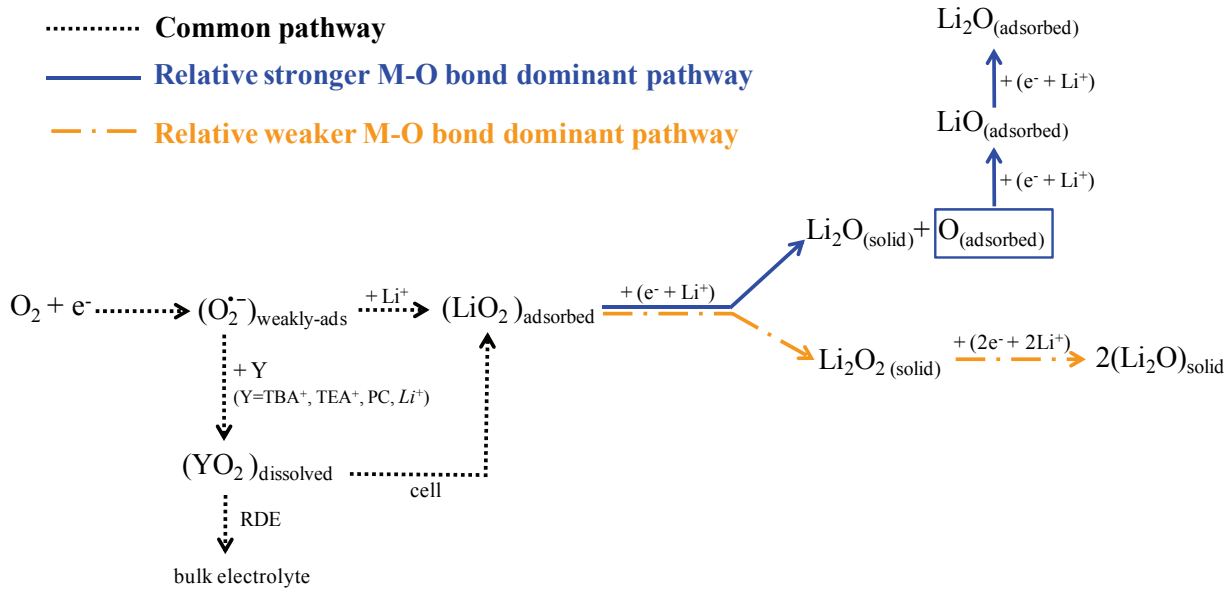

Figure S7. ORR mechanism for Li^+-containing nonaqueous solvents (Reference 7)[7]

The ORR activity trend in nonaqueous and alkaline electrolytes

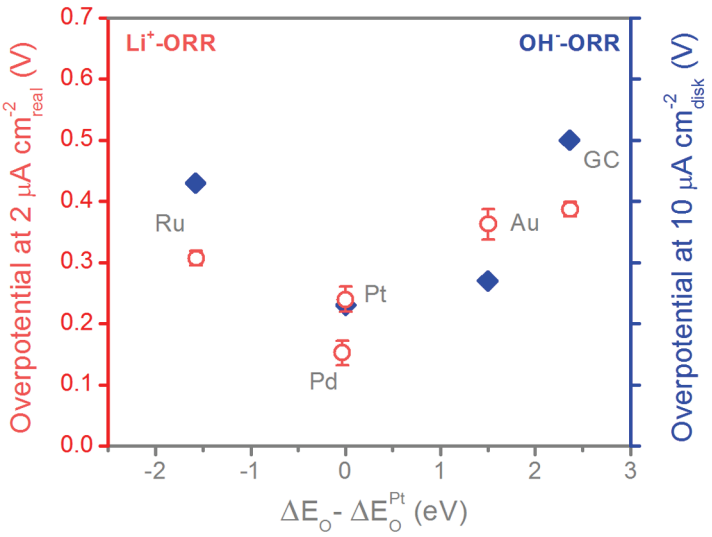

Figure S8. The overpotentials of the nonaqueous Li^+-ORR at 2 μA cm^{-2}_{real} and alkaline OH^--ORR at 10 μA cm^{-2}_{disk} (Ru is estimated from Ref 8) as a function of calculated oxygen adsorption energy, ΔE_O[9,10].

References

(1) Aurbach, D., Daroux M.L., Faguy P. and Yeager E. *J. Electroanal. Chem.* **1991**, 297, 225.

(2) Gasteiger, H. A.; Markovic, N. M.; Ross, P. N. *J. Phys. Chem.* **2002**, 99, 16757.

(3) Green, C. L.; Kucernak, A. *J. Phys. Chem. B* **2002**, 106, 1036.

(4) Chierchie, T.; Mayer, C.; Lorenz, W. J. *J. Electroanal. Chem.* **1982**, 135, 211.

(5) Tremiliosi-Filho, G., Dall'Antonia, L.H., Jerkiewicz, G. *J. Electroanal. Chem.* **1997**, 422, 149.

(6) Kinoshita, K. *Carbon: Electrochemical and Physicochemical Properties*; 1st ed.; Wiley-Interscience: New York, 1988.

(7) Lu, Y.-C.; Gasteiger, H. A.; Crumlin, E.; McGuire, J. R.; Shao-Horn, Y. *J. Electrochem. Soc.* **2010**, 157, A1016.

(8) Lima, F. H. B.; Zhang, J.; Shao, M. H.; Sasaki, K.; Vukmirovic, M. B.; Ticianelli, E. A.; Adzic, R. R. *J. Phys. Chem. C* **2007**, 111, 404.

(9) Hammer, B.; Norskov, J. K. *Adv. Catal.* **2000**, 45, 71.

(10) Sorescu, D. C.; Jordan, K. D.; Avouris, P. *J. Phys. Chem. B* **2001**, 105, 11227.